Physiological Properties of Inhibitory Interneurons in Cat Striate Cortex

Rony Azouz[1], Charles M. Gray[1,2], Lionel G. Nowak[3] and David A. McCormick[3]

[1]Center for Neuroscience, [2]Section of Neurobiology, Physiology and Behavior, University of California, Davis, CA 95616 and [3]Section of Neurobiology, Yale University School of Medicine, 333 Cedar Street, New Haven, CT 06510, USA

Physiological and morphological properties of identified interneurons in the striate cortex of the cat were studied *in vivo* by intracellular recording and staining with biocytin. In conformity with *in vitro* studies, these non-pyramidal fast spiking cells have very brief action potentials associated with a high rate of fall, and a large hyperpolarizing afterpotential. These cells show high discharge rates, little or no spike frequency adaptation in response to depolarizing current injection, as well as a diverse range of firing patterns. Three of the cells were labeled and were found to be aspiny or sparsely spiny basket cells, with bitufted or radial dendritic arrangements, in layers II–IV. Their axonal arborizations were more dense near their somata and extended horizontally or vertically. Of 13 visually responsive cells tested, the receptive field properties of six cells and the orientation and direction preferences of eight cells were determined. Five of the successfully mapped cells had simple receptive fields while one had a complex receptive field type. The orientation and direction tuning properties of the overlapping set of eight cells showed a broad spectrum ranging from unselective to tightly tuned. The majority exhibited a clear preference for orientation and none of the cells were clearly direction selective. Quantitative analysis of the temporal properties of the spike trains during visual stimulation and spontaneous activity revealed that these cells do not exhibit any significant periodic activity, and fired at rates that were well below their maximum in response to depolarizing current pulses.

Introduction

GABAergic inhibitory interneurons play a major role in shaping the functional properties of visual cortical cells (reviewed in Sillito, 1984; Martin, 1988; Chapman and Stryker, 1992; Eysel, 1992; Berman *et al.*, 1992; Vidyasagar *et al.*, 1996). Despite their prevalence and essential role in cortical function, only a few studies have examined their physiological properties directly. This is largely due to technical limitations: intracellular recording from identified interneurons *in vivo* is the only technique that permits a direct examination of their functional properties. Consequently the study of neocortical inhibitory interneurons has been largely restricted to the *in vitro* slice preparation. These studies have revealed the intrinsic electrophysiological properties of these neurons as well as their important role in the regulation of neuronal excitability (McCormick *et al.*, 1985; Jones and Heinemann, 1988; Foehring *et al.*, 1991; Llinàs *et al.*, 1991; Jones and Bühl 1993; Kawaguchi, 1995; Chen *et al.*, 1996a; Kawaguchi and Kubota, 1996, 1997; Tasker *et al.*, 1996; Thomson *et al.*, 1996; Thomson and Deuchars, 1997). Although this technique has clear advantages for studying the cellular properties of interneurons, it has obvious limitations for investigating physiological function. In a few studies, intracellular recording and staining *in vivo* has demonstrated that non-spiny interneurons exhibit both simple and complex receptive fields, are responsive to input from one or both eyes, and are often tuned for orientation and occasionally direction of movement (Gilbert and Wiesel, 1979; Lin *et al.*, 1979; Martin *et al.*, 1983, 1989; Martin, 1984, 1988; Kisvárday *et al.*, 1987; Gabbott *et al.*, 1988; Anderson *et al.*, 1993; Ahmed *et al.*, 1997).

Most of the physiological information concerning inhibition, however, has been extrapolated from extracellular recordings employing a variety of stimulus paradigms (Hubel and Wiesel, 1962; Bishop *et al.*, 1971; Henry *et al.*, 1974; Orban, 1984) or pharmacological manipulations (Sillito, 1977; Bolz and Gilbert, 1986; Eysel *et al.*, 1990; Crook *et al.*, 1992, 1996). These studies have shown that the selective receptive field properties of cortical neurons, such as orientation and direction selectivity, subfield antagonism and end stopping, are mediated in part by inhibitory processes (Bishop *et al.*, 1971; Orban *et al.*, 1979; Morrone *et al.*, 1982; Bolz *et al.*, 1986; Grieve *et al.*, 1991). A more direct approach, using intracellular recording *in vivo,* has enabled the study of inhibition by investigating membrane potential (Vm) changes of presumed excitatory neurons in response to electrical and visual stimulation (Ferster, 1986, 1988; Berman *et al.*, 1991; Douglas *et al.*, 1988, 1991; Vidyasagar *et al.*, 1996). These findings further support the hypothesis that GABAergic mechanisms are involved in the generation of receptive field properties, although the precise mechanisms are not fully understood. A direct investigation of activity in the inhibitory interneuron population might yield new insights into the functional role of inhibition.

Such an approach might also help to elucidate the mechanisms controlling response synchronization, a form of activity hypothesized to contribute to visual feature integration (Singer and Gray, 1995). Recent studies have demonstrated that some cortical neurons exhibit synchronized oscillations in the gamma frequency range (30–70 Hz) in response to visual stimulation (Gray and Singer, 1989; reviewed in Gray, 1994; Singer and Gray, 1995). Numerous theoretical and experimental studies have suggested that inhibition may play a crucial role in the generation of this synchronous rhythmic activity (Wilson and Cowan, 1972; Freeman, 1975; Konig and Schillen, 1991; Llinas *et al.*, 1991; Bush and Douglas, 1991; Lytton and Sejnowski, 1991; Bush and Sejnowski, 1996). Although there is some support for this hypothesis from the hippocampal formation (Jeffreys *et al.*, 1996; Traub *et al.*, 1996), the contribution of inhibition to visual cortical gamma-band activity remains unclear.

In the present study, we obtained direct evidence for the functional properties of inhibitory interneurons in cat striate cortex using a combination of intracellular recording and staining *in vivo*. On the basis of previous *in vitro* studies (McCormick *et al.*, 1985), we have focused our efforts on so called fast spiking (FS) cells that have at least three distinct intrinsic characteristics: very brief action potential duration, little or no spike frequency adaptation in response to

intracellular depolarizing current injection, and a steep linear relationship between discharge frequency and amplitude of current injection. Cells having these properties have been shown to correlate well with the morphological characteristics of a subset of GABAergic interneurons, including basket cells and chandelier cells (McCormick *et al.*, 1985; Naegele and Katz, 1990; Kawaguchi and Kubota, 1993, 1997; Jones and Bühl 1993; Tasker *et al.*, 1996). Here we determine the intrinsic membrane properties, responses to visual stimuli, receptive field properties, and selectivity for stimulus orientation and direction of fast spiking interneurons in the cat primary visual cortex.

Materials and Methods

Adult cats (2.5–4.0 kg) were initially anesthetized with ketamine (12–15 mg/kg) and xylazine (1 mg/kg) and given atropine (0.05 mg/kg) to reduce salivation. Ringer solution containing 2.5% dextrose was given i.v. throughout the experiment (4 ml/kg/h). Anesthesia was maintained using Halothane (1.0–1.5%), in a mixture of nitrous oxide and oxygen 2:1, while the animals were actively ventilated. The EKG, heart rate (160–200 bps), expiratory CO_2 concentration (3.5–4.5%) and rectal body temperature (37.5–39.0°C) were monitored throughout the experiment. The animals were mounted in a stereotaxic frame. In order to minimize pulsations arising from the heartbeat and respiration, the cisterna magna was cannulated, a bilateral pneumothorax was performed, and the animal was suspended by the rib cage to the stereotaxic frame. A craniotomy (3–4 mm) was made overlying the representation of the area centralis of area 17. Following the surgery, the animals were paralyzed with pancuronium bromide (Pavulon, 3 mg/kg initial bolus followed by 3 mg/kg/h). The eyes were focused on the screen of a computer monitor at a distance of 57 cm using corrective, gas-permeable contact lenses. The nictitating membranes were retracted and the pupils dilated using ophthalmic neosynephrine and atropine, respectively. Following these procedures, a small opening was made in the dura, and a micropipette was positioned just above the cortical surface. Stability was further improved by application of a 4% mixture of agar in Ringer solution to the cortical surface. Within 10–12 h of recording and staining of the first cell, each animal was given a lethal injection of Nembutal and perfused through the heart with phosphate-buffered saline (PBS), followed by PBS containing 2% paraformaldehyde and 1.25% glutaraldehyde.

Intracellular recordings were obtained using potassium acetate (1.2 M) and 2% biocytin-filled glass micropipettes beveled to a final resistance of 70–120 MΩ. After each recording, the depth of the electrode tip was noted and the position of the recording site was marked on the skull. A new site was chosen at least 1 mm away from the previous recording site and the entire procedure was repeated. The intracellular signals were stored on a digital tape recorder, and digitized off-line at a rate of 20–50 kHz. The cortical cells accepted for this study had stable membrane potentials ranging from –80 to –55 mV and action potentials of 50–90 mV amplitude.

Visual stimuli consisted of drifting light bars or square-wave gratings (2–5 cd/m^2) presented on a dark background. The stimuli were generated by a personal computer and displayed on a 19 in. color monitor (80 Hz non-interlaced refresh, 1024 × 768 resolution).

For each cell, we computed several parameters of the action potentials extracted from the cell's responses to depolarizing current pulses. These parameters included the action potential width at half amplitude, the maximum rate of rise and fall in action potential voltage, the magnitude of the fast afterhyperpolarization (AHP) following each spike, the absolute refractory period (estimated by the minimal interspike interval), and the frequency versus current slope (*f*–*I*). The spike trains collected during spontaneous activity and in response to visual stimuli were quantified with the following measures: the peristimulus–time histogram (PSTH), the autocorrelation histogram (ACH), the power spectrum of the ACH using the fast Fourier transform (Press *et al.*, 1992), the interspike interval histogram (ISIH) and the direction tuning curve. The presence or absence of rhythmicity in the spike trains was evaluated using previously published methods (Gray and Viana Di Prisco, 1997). Rhythmic activity induced in the spike trains as a consequence of the refresh rate of the computer monitor was assessed by computing the shift

predictor control correlogram. The membrane potentials were processed for further analysis by selecting two epochs from each trial, one during the period of spontaneous activity and the other during the visual response. For both epochs, the action potentials were removed using a median filter and the resulting data stored at a resolution of 1 kHz.

To determine if the spike activity of each cell was tuned for orientation, we fit a Gaussian function, using the maximum likelihood method (Maldonado and Gray, 1996), over the 180° range of the direction tuning curve that elicited the maximal response. We assessed the responsiveness of each cell to the stimuli by performing a Student's *t*-test between the peak value of the tuning curve and its corresponding value of spontaneous activity. To assess the quality of the fit, we compared the Gaussian fit to that of a straight line at the mean amplitude level of the same tuning curve. Cells were considered tuned for orientation using this measure if the tuning curve was significantly better fit by the Gaussian function. From the Gaussian fit of each cell, we estimated the orientation preference (peak) and the orientation bandwidth (σ of Gaussian). We further evaluated the orientation selectivity of the cells by assigning each with an orientation index (OI) according to the formula:

$$OI = \frac{R_P - R_M}{R_P}$$

where

R_P = (response to the preferred orientation) – (mean level of maintained activity)

R_M = (minimal response to a non-preferred orientation) – (mean level of maintained activity)

We operationally defined the orientation selectivity of cells according to the following criteria:

orientation selective: [$OI > 0.85$] and [σ < 45°]
orientation biased: [$0.85 > OI > 0.5$] and [45° < σ < 60°]
unselective: [$0.5 > OI$] and [σ > 60°]

These criteria were based on a previous study employing a similar orientation index (Hawken and Parker, 1984) and on two recent studies in our laboratory using the Gaussian fitting method (Maldonado and Gray, 1996; Maldonado *et al.*, 1997). In the latter studies, it was demonstrated that the mean bandwidth of tuned neurons in cat striate cortex is 30° ± 15° (SD).

We also evaluated the direction selectivity of each cell by assigning each with a direction index (*DI*) (Albus, 1980) according to the formula:

$$DI = 1 - \frac{R_N}{R_P}$$

where:

R_P = (response to the preferred direction) – (mean level of maintained activity)

R_N = (response to the null direction) – (mean level of maintained activity)

This index normally ranges in value from 0 to 1. Values >1 occur when the response to the null direction is inhibitory with respect to the maintained activity. We considered cells with $DI < 0.5$ to be unselective for direction, those with $0.5 < DI < 0.75$ to be direction biased, and those with $DI > 0.75$ to be direction selective.

For histology, a block of tissue containing the filled cells was sunk in 30% sucrose. Coronal sections were cut at 60–80 µm thickness and reacted for the presence of biocytin using standard techniques and diaminobenzidine visualization. Sections were mounted on glass slides, dehydrated and coverslipped. Sections adjacent to those containing labeled cells were stained with cresyl violet to reveal laminar boundaries. Cells were photographed digitally at low power for overall morphology and then at high power with a 100× oil immersion lens using a differential
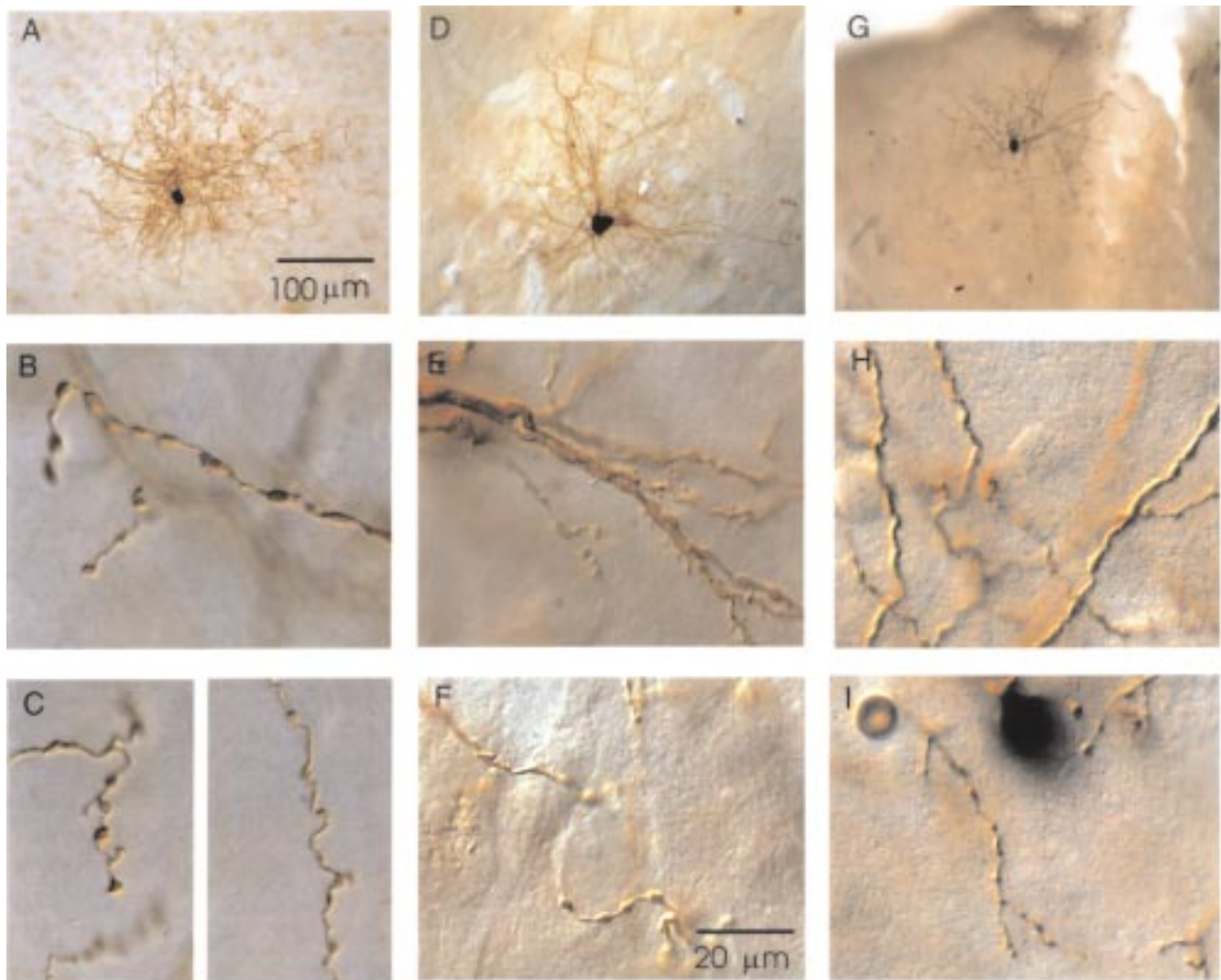
Figure 1. Photomicrographs of three identified interneurons filled with Biocytin. (*A*) A fast spiking cell with dendritic and axonal innervation largely restricted to layer IV. This cell is morphologically similar to a 'clutch' type of basket cell, and is illustrated on the cover of this issue. (*B*) The dendrites of the cell in *A* at a higher resolution appear beaded and aspiny. (*C*) The axon of this cell gives rise to numerous 'en passant' synaptic boutons. (*D*) A sparsely spiny basket cell located in layer III. (*E*) The dendrites of the cell in *D* at a higher resolution. Note the presence of dendritic spines. (*F*) The axon of this cell is beaded and displays numerous 'en passant' boutons that occasionally give rise to repeated putative synaptic terminations on the somata of other neurons. (*G*) A small layer II aspiny fast spiking cell. This cell appears morphologically similar to a small basket cell. The white space next to the labeled cell represents a blood vessel. (*H*) The dendrites of the cell in *G* at a higher resolution. (*I*) Axonal branches of the cell shown in *G* and *H*. Scale bar in *A* for *A*, *D* and *G*. Scale bar in *F* for *B*, *C*, *E*, *F*, *H* and *I*.

interference contrast (DIC) microscope. Measurements were not corrected for tissue shrinkage.

Results

The results of this study were taken from 15 FS neurons that were selected from a larger sample of over 150 intracellular recordings. The cells had stable membrane potentials for durations of 20–90 min. Thirteen of the cells were sufficiently visually responsive that we were able to map their receptive field locations and record their responses to visual stimuli. These cells had three distinct intrinsic characteristics that immediately distinguished them from the other cells that we encountered. Their action potentials were very brief in duration, they displayed relatively little spike frequency adaptation in response to depolarizing current injection, and they exhibited a steep linear relationship between injected current and action potential frequency. These properties suggested that they belonged to the

previously established class of neurons known as FS cells (McCormick *et al.*, 1985). Injection of biocytin into three of these neurons revealed a distinct set of morphological features characteristic of inhibitory interneurons. In addition to these features, we investigated the discharge patterns and receptive field properties of these cells and the results are described in detail in the following sections.

Morphological Features

Three morphologically identified interneurons were recovered following intracellular injection of biocytin (Fig. 1*A,D,G*). These neurons were clearly non-pyramidal, and were aspiny or sparsely spiny cells with beaded dendrites. The soma of one labeled cell (Fig. 1*A*–*C*) was located at the bottom of layer IV and was ~14 × 19 μm in diameter. Its dendrites had a smooth but beaded appearance (Fig. 1*B*) and extended 270 μm parallel to the cortical surface and 225 μm along the pia–white matter axis.
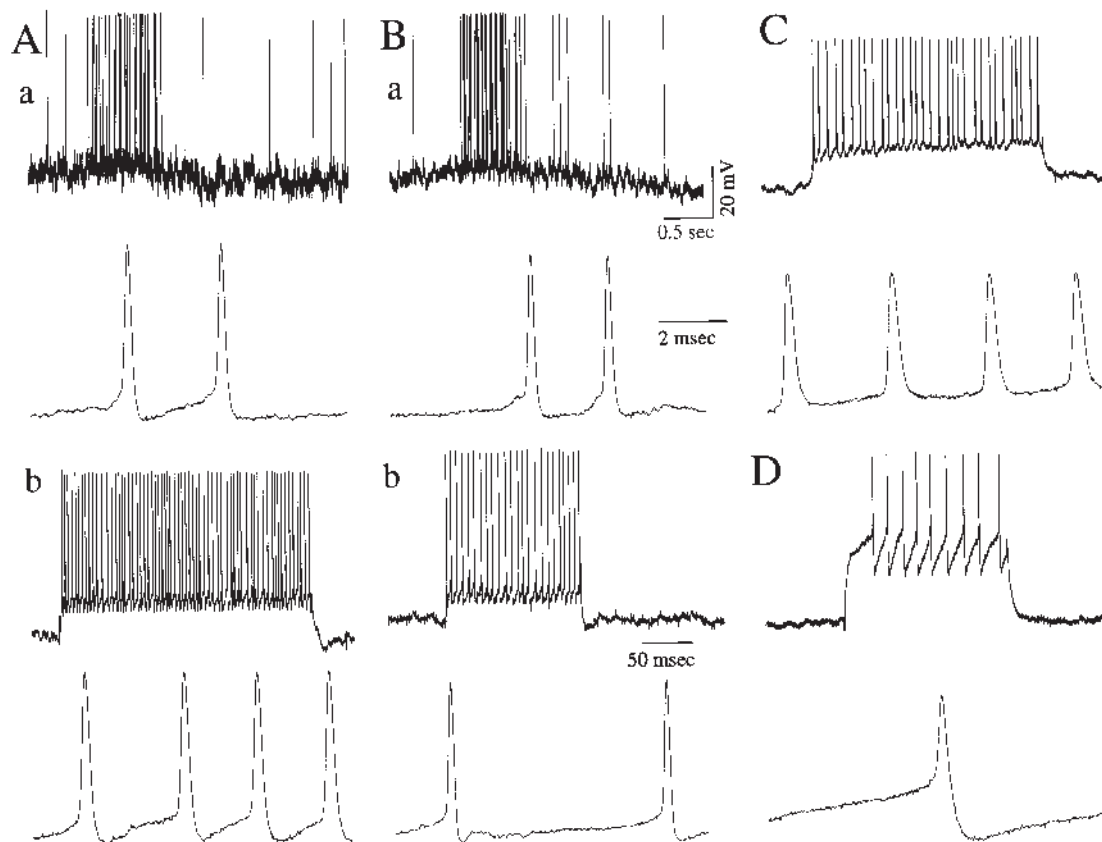
Figure 2. Visual and intrinsic responses of four different fast spiking cells. The cells shown in *A*, *B* and *C* correspond to the three cells shown in *A*, *D* and *G* of Figure 1, respectively. The cell shown in *D* exhibits some distinct intrinsic characteristics and is shown for the purpose of comparison. The plots in *A* and *B* show the responses to a visual stimulus (*a*) and a depolarizing current pulse (*b*). The lower plots in panels *A–D* show the action potentials in more detail. The cell shown in *A* was monocular and broadly tuned for orientation. It was activated by a drifting bar. The cell shown in *B* was binocular and direction selective. It was activated by a drifting bar presented to the left eye. The cell shown in *C* was not tested with visual stimuli. The cell shown in *D* displayed a late onset in spike activity suggesting that it may correspond to the late-spiking category described by Kawaguchi *et al.* (1996). Note that in response to a strong depolarizing current pulse the cells in *A–C* exhibit high sustained firing rates with little or no spike frequency adaptation.

This cell possessed a densely branching axonal arbor, having numerous 'en passant' synaptic boutons (Fig. 1*C*), that primarily innervated the region bounded by the dendritic tree, but also extended ~460 μm in the plane of layer IV. A few branches projected superficially, but stayed largely within layer IV, giving the axonal arbor a total extent of 620 μm perpendicular to the cortical surface. The morphological features of this cell are similar to those previously described for the 'clutch' subtype of basket cell in layer IV of cat visual cortex (Kisvárday *et al.*, 1985).

Another labeled cell (Fig. 1*D–F*), located in layer III, had characteristics consistent with those of large basket cells (Kisvárday *et al.*, 1993). Its soma was 20 × 22 μm in diameter, and it possessed sparsely spiny, beaded dendrites (Fig. 1*E*) that extended 370 μm in the plane of layer III and 380 μm perpendicular to the cortical surface. This cell had a densely branched local axonal projection as well as a patchy lateral projection in layers II/III extending >1200 μm from one end of the axonal arbor to the other. The axon also projected vertically in a columnar fashion into layer V as well as extending branches into layer II. The axon did not appear to have any terminals that entered layer I and its vertical extent was ~920 μm. As shown in Figure 1*F*, the axon displays numerous 'en passant' boutons and appears to make multiple synaptic contacts onto the somata of other cells. These features are characteristic of a classic basket cell. Its only novel feature was the presence of spines on its

Table 1
Action potential properties of fast spiking cells

	n = 15
Fast AHP (mV)	10.10 ± 1.32
Spike width 1/2 amplitude (ms)	0.32 ± 0.06
Max rate of rise (V/s)	411.2 ± 109.9
Max rate of fall (V/s)	292.39 ± 68.0
Minimal ISI (ms)	1.85 ± 1.45
f–I slope primary (Hz/nA)	384.48 ± 173.52

All data expressed as mean ± SD.

dendrites, although this property has been described previously (Peters and Regidor, 1981).

The third cell (Fig. 1*G–I*) was located in layer II. Its cell body was small, measuring 10 × 12 μm in diameter. The dendrites of this cell were smooth and beaded in appearance (Fig. 1*H*), were located primarily in layer II, and extended ~200 μm in the plane of layer II. The cell gave rise to a local axonal projection that extended beyond the dendritic arbor ~800 μm parallel to the cortical surface. Both the axon and dendrites extended into layer I and the axon appeared to make 'en passant' synaptic contacts onto other neurons. The morphological features of this cell suggest that it may be a small basket neuron (DeFelipe *et al.*, 1982).
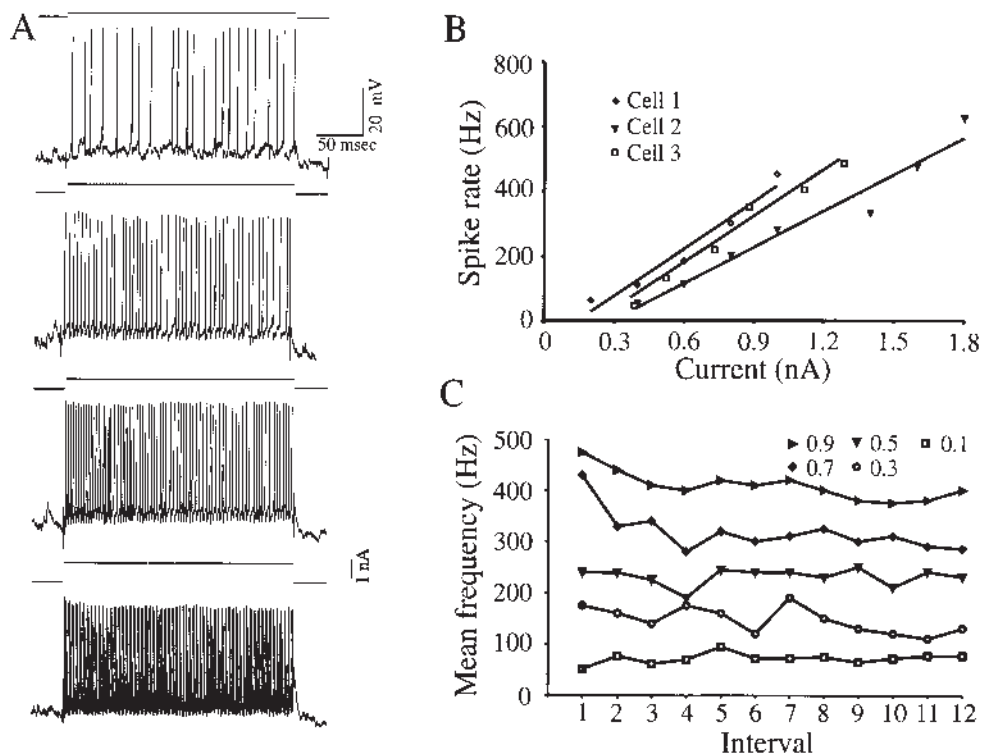
Figure 3. Response characteristics of FS cells to depolarizing current pulses of varying magnitude. (*A*) Responses displayed by an FS cell to different levels of depolarization. (*B*) Action potential frequency versus current (*f–I*) plots for three FS cells. The firing rates were computed from the first interspike interval. (*C*) Spike frequency versus interval number for the cell illustrated in (*A*). The magnitude of injected current is indicated by the different symbols. Note the minor amount of adaptation at higher current intensities.

Intrinsic Properties

We evaluated the intrinsic properties of all the cells (*n* = 15) by calculating several parameters of the action potential discharges in response to depolarizing current pulses. These data, shown in Table 1, demonstrate that FS cells recorded *in vivo* have intrinsic properties similar to the class of nonpyramidal FS cells documented previously *in vitro* (McCormick *et al.*, 1985). Their action potentials were very brief in duration and were often preceded by a slow depolarizing ramp (5–50 ms in duration) which was more apparent during low firing rates (Fig. 2*Aa*). The rate of repolarization of the action potentials was comparatively high and each spike was typically followed by a brief (3–12 ms), but prominent (5–12 mV), hyperpolarizing afterpotential (Fig. 2). Their peak firing rates, as expressed by the minimal interspike interval, were >500 Hz. They displayed a steep linear relation between depolarizing current and spike frequency. And, except for a brief slowing after the initial few spikes, the discharge rates of these cells showed little if any spike frequency adaptation during depolarizing current pulses lasting 100–200 ms (Fig. 3*A*).

In addition to these well-established properties of FS cells, we also recorded from three neurons that displayed long spike latencies in response to depolarizing current pulses. These spikes were preceded by slowly developing ramp depolarizations (Fig. 2*D*). This property was suggestive of a distinct subclass of interneurons as recently demonstrated *in vitro* (referred to as late spiking cells: Kawaguchi, 1995; Kawaguchi and Kubota, 1997). However, because we could find no other physiological properties that distinguished these FS cells as potentially being unique, they were grouped together with the other FS neurons.

Table 2
Inter-spike interval properties of fast spiking cells

	1 Spontaneous *n* = 13	2 Drifting light bar *n* = 13	3 Drifting grating *n* = 6
Minimal ISI (ms)	6.4 ± 4.7[*2,3]	2.5 ± 1.7[*1,3]	1.7 ± 1.2[*1,2]
Mean ISI (ms)	50.2 ± 16.7[*2,3]	30.4 ± 8.3[*1,3]	24.1 ± 8.6[*1,2]
Mode ISI (ms)	14.2 ± 13.6	8.6 ± 5.1	9.2 ± 4.8
ISI 5 (%)	3.9 ± 5.6[*2,3]	9.8 ± 12.8[*1]	16.8 ± 20.0[*1]

All data expressed as mean ± SD. Kolmogorov–Smirnov test performed to compare differences between spontaneous and different visual stimuli.

ISI 5, the percentage of ISIs occurring during the visual response or spontaneous activity that were below and equal to 5 ms.

*Significantly different ($P < 0.05$) from the indicated group.

Discharge Characteristics Evoked by Visual Stimulation

For most of the cells in our sample (*n* = 13), we were able to record long enough to assess their discharge characteristics preceding and during the presentation of visual stimuli. For each cell, these properties were evaluated by computing the mean firing rate, the ACH and its corresponding power spectrum, and several parameters quantifying the ISIH (Table 2). As a group these cells displayed relatively uniform patterns of spontaneous and stimulus-evoked discharges. On average, the spontaneous and visually evoked mean discharge rates of the cells were typical of those encountered among most cortical neurons (spontaneous = 7.6 ± 8.9 s/s; drifting light bar = 19.2 ± 11.7 s/s; drifting grating = 36.6 ± 11.34 s/s). Interestingly, this indicates that the stimuli used here evoked responses that were a small fraction of the maximum discharge rates attainable by
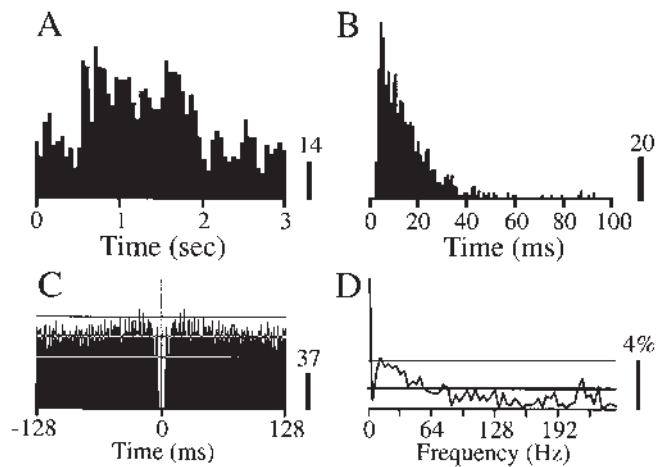
Figure 4. Discharge characteristics of an FS cell in response to an optimal visual stimulus. The cell had a simple receptive field and was direction biased. (*A*) PSTH recorded in response to 30 presentations of an optimally oriented drifting light bar presented to the contralateral eye. (*B*) The ISIH computed from the spike train sampled during the visual response. (*C*) The ACH computed from the spike train sampled during the visual response. The middle horizontal bar indicates the mean value of the trial-shuffled correlogram while the upper and lower lines denote the mean ± 2 SD. The calibration bar at the lower right of *A*–*C* indicates the number of spikes. (*D*) Fourier power spectrum of the ACH shown in *C*. The thick horizontal line indicates the mean power of the corresponding pseudo-random spike train while the thin line indicates the mean + 3 SD. Note that the spectrum of the ACH shows no evidence of periodicity. The calibration bar in *D* represents the percentage of power with respect to the peak value at the DC level.

these cells. The ISIHs of these cells exhibited a broad range of interspike intervals that were distributed in a unimodal fashion and displayed relatively low percentages of intervals <5 ms in duration, indicating that they rarely fired in high–frequency bursts. The ACHs and their associated power spectra showed no evidence of periodic firing. Figure 4 shows the results of these calculations for a cell that is representative of our sample as a whole. The cell was stimulated with a drifting light bar, and the calculations were performed on a data segment 1.0 s in duration centered on the response to the visual stimulus. Similar to the other cells in our sample (*n* = 13), this cell exhibited a unimodal distribution of interspike intervals and did not exhibit any obvious periodicity in the ACH. When a subset of the same cells (*n* = 6) was stimulated with drifting square-wave gratings, we observed an increase in the percentage of short intervals, but this effect did not alter the basic shape of either the ISIH or the ACH. We did observe, however, that two of the neurons activated by the grating stimuli exhibited 80 Hz oscillations that were time-locked to the stimulus and were driven by the video refresh (80 Hz) of the computer monitor. This was indicated by the presence of significant peaks in the shift predictor correlogram. Overall, the relative lack of high-frequency burst firing and periodicity clearly distinguishes FS cells from a recently described class of neurons called 'chattering cells' that also exhibit very brief action potential durations (Gray and McCormick, 1996). Figure 4 shows the results of these calculations for a cell that is representative of our sample as a whole. The cell was stimulated with a drifting light bar, and the calculations were performed on a data segment 1.0 s in duration centered on the response to the visual stimulus. Similar to the other cells in our sample (*n* = 13 total), this cell exhibited a unimodal distribution of interspike intervals and did not exhibit any obvious periodicity in the ACH.
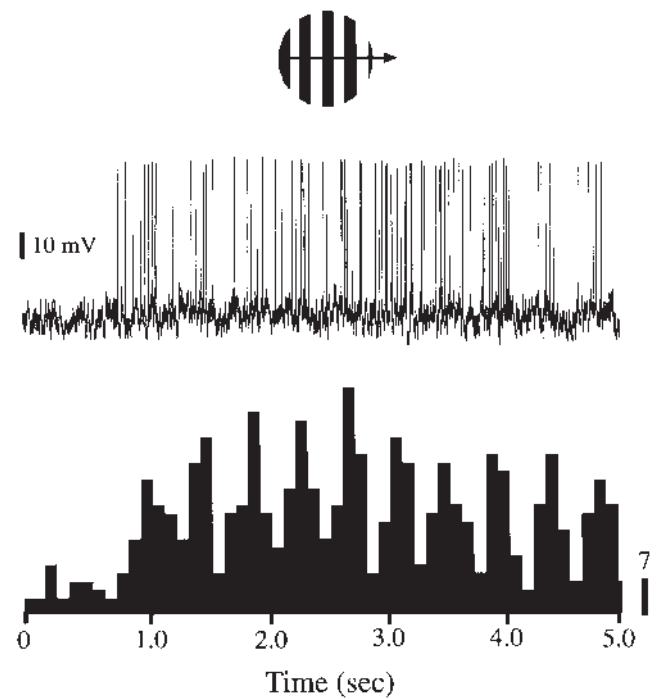

Figure 5. Response of an FS cell with a simple RF to a drifting square-wave grating (0.8 cycles/deg). The upper panel depicts the membrane potential of the cell recorded during a single presentation of the stimulus. The lower panel illustrates the PSTH recorded in response to 20 presentations of the same stimulus. The calibration bar at the lower right of the lower panel indicates the number of spikes.

Table 3
Orientation and direction tuning of fast spiking cells

Cell number	Spontaneous level (%)	Minimal response (%)	σ (deg)	Direction index	Orientation index
1	0.6	11.7	27.63	0.67[E]	0.89[A]
2	4.3	11.2	29.12	0.64[E]	0.93[A]
3	0.6	22.7	46.65	0.48[F]	0.78[B]
4	0.4	1.0	31.82	0.46[F]	0.99[A]
5	0.7	0	44.15	0.39[F]	1.0[A]
6*	4.2	56.2	77.4	0.39[F]	0.45[C]
7	0.4	7.5	34.57	0.28[F]	0.92[A]
8	0.7	0	19.61	0.1[F]	1.0[A]

Percent (%) refers to the percentage of the maximal response in the tuning curve.

Minimal response is the response to the least effective orientation. These values have been corrected by subtracting the magnitude of the spontaneous activity preceding the stimulus.

*The morphology of this cell is illustrated in Figure 1*A*.

A, orientation selective; B, orientation biased; C, orientation untuned; D, direction selective; E, direction biased; F, direction untuned.

Receptive Field Properties

In addition to their discharge properties, we were able to determine the receptive field properties of a subset of the FS cells. For some cells this was accomplished by mapping the location of ON and OFF subfields using a flashing light bar. Others were stimulated with a drifting square-wave grating at optimal spatial and temporal frequency in order to test for the presence of modulated responses indicative of simple receptive fields (Maffei and Fiorentini, 1973; Movshon, 1978a,b; Skottun *et al.*, 1991). Of the six cells unambiguously classified, five had 'simple' and one had 'complex' receptive field properties. Figure 5 shows the response of one of these cells to a drifting
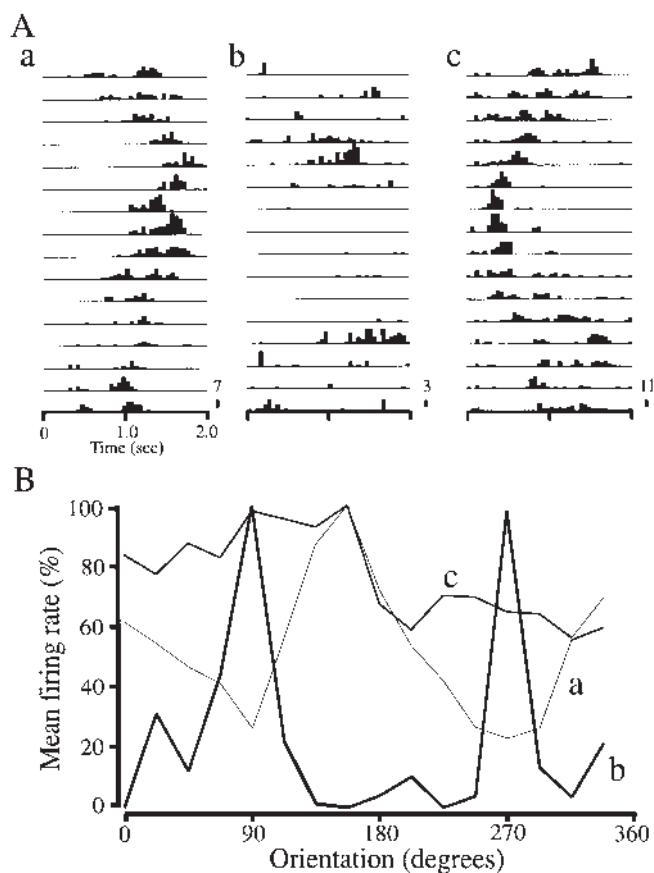
Figure 6. Examples of three FS cells exhibiting wide variation in their orientation tuning. (*A*) PSTHs for the three neurons (*a–c*). The cells were stimulated by a drifting light bar presented over a range of 360° at a resolution of 22.5°. The calibration bar at the lower right of each PSTH column indicates the number of spikes. (*B*) Normalized tuning curves for the same three neurons computed from the mean firing rate sampled from a temporal window centered on the peak of each visual response. Note that cell *a* is orientation biased, cell *b* is orientation selective and cell *c* is untuned. The morphology of the cell represented by curve *c* is shown in Figure 1*A*.

Figure 7. The membrane potential fluctuations of FS cells exhibit broader tuning for orientation and direction than their spike activity. *A* and *B* show examples of the direction tuning curves for action potential discharges (thick lines) and membrane potential fluctuations (thin lines).

square-wave gratings. The clear modulation of the response at the temporal frequency of the gratings (0.8 cycles/deg) was consistent with the classification of this cell as simple.

In addition to the receptive field type, we also quantitatively mapped the direction and orientation tuning profile of the action potential discharges of eight of the FS cells. The responses of these cells ranged from being tightly tuned for orientation and direction biased to showing no selectivity for either parameter. The cumulative results of our analysis are given in Table 3 and selected examples of the tuning profiles for three cells are shown in Figure 6. Six out of eight cells in our sample were orientation selective. Of the remaining two cells, one cell was broadly tuned (orientation biased) and another showed no selectivity for orientation (unselective). Only two of the cells were direction biased, while the remaining six cells showed no selectivity for stimulus direction. Interestingly, we found that even though most of these cells exhibited a high degree of orientation selectivity, five out of the eight cells in this study showed a significant response to all orientations as expressed in the minimal response in the orientation tuning curve (mean = 21.7 ± 20.0%).

We further investigated the membrane potential changes underlying the orientation and direction tuning in these cells. This was accomplished by computing the mean membrane
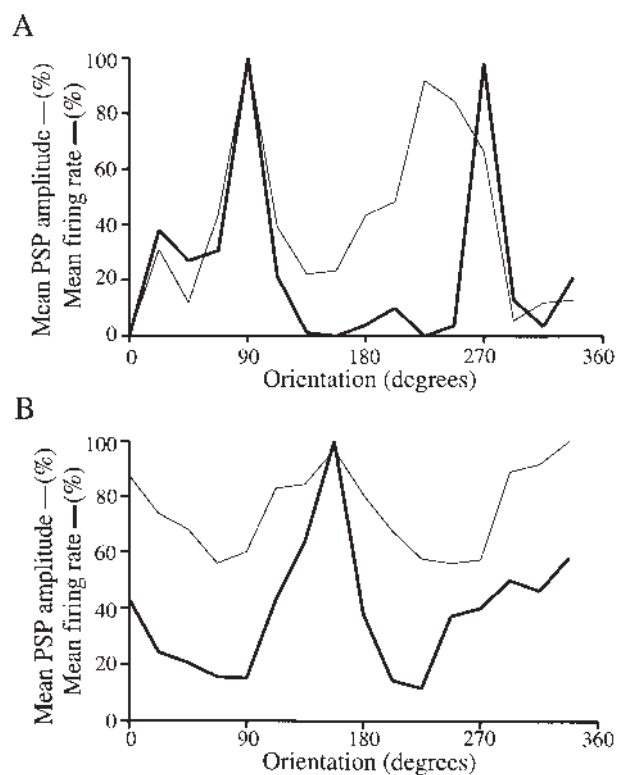
potential of the cells during the response to the visual stimuli after having removed the action potentials from the records using a median filter. In all the neurons studied, the orientation tuning curves computed from the postsynaptic potentials (PSPs) were broader and less selective than those computed from the firing rates. Figure 7 shows two representative examples of the tuning curves computed from both the PSPs and the spike discharges. In both examples, the PSPs are more broadly tuned than the corresponding discharge rates. The cell in Figure 7*A* actually displays a difference in the preferred orientation between the PSPs and the firing rates. The tuning curves shown in Figure 7*B* illustrate the more typical result where the PSPs are more broadly tuned, but coincide with the spike discharges of the cell.

Discussion

The aim of this study was to determine the functional properties of inhibitory interneurons in cat striate cortex. Although previous efforts have focused on extracellular recordings from presumed interneurons (e.g. Swadlow, 1988) or the morphological identification of each cell recorded (e.g. Martin, 1988; Table 4), we attempted to classify the properties of a subset of GABAergic interneurons that were identified by the correlation between their intrinsic electrophysiological and morphological characteristics. Examination of the morphology of the cells in the present study, as well as previous investigations, have revealed that FS neurons are consistently associated with several subtypes of GABAergic non-pyramidal neurons including basket cells and chandelier cells (McCormick *et al.*, 1985; Kawaguchi and Kubota, 1993, 1997; Thomson and Deuchars, 1997). We

Table 4
Receptive field properties of morphologically identified interneurons

Morphological type	Layer	Receptive field type	Orientation selective	Direction selective	Ocular dominance	Animal	Reference
Basket	IVA	S_2	yes	pref.	7	cat	1
Basket	III	C_{SP}	yes	yes	4	cat	1
Basket	III	S_2	yes	NA	4	cat	1
Clutch	IVB	C_{ST}	yes	NA	6	cat	1
Multipolar	I	S	yes	no	4	cat	3
Clutch	IV	S_2	yes	NA	7	cat	4
Multipolar	IV	S	NA	NA	NA	cat	5
Basket	V	S	yes	NA	NA	cat	6
Smooth Stellate	II/III	S	NA	NA	NA	cat	7
Double Bouquet	II/III	S_1	yes	NA	NA	cat	8
Basket	IVA	S_1	yes	pref.	7	cat	9
Basket	IVA	S_1	yes	pref.	7	cat	9
Basket	IVA	S_2	yes	pref.	3	cat	9
Basket	IVA	C_{ST}	yes	pref.	7	cat	9
Basket	II	C	NA	NA	2	monkey	2
Chandelier	II	S_1	yes	yes	2	monkey	2
Basket	VI	S_2	NA	NA	4	monkey	2
Clutch	IVA	NA	no	NA	1	monkey	2

NA, not available; C, complex; S, simple; C_{ST}, standard complex; C_{SP}, special complex; S_1, simple cells with one subfield (either ON or OFF); S_2, simple cells with two subfields (ON and OFF).

References: 1, Martin *et al.* (1983); 2, Anderson *et al.* (1993); 3, Martin *et al.* (1989); 4, Gabbott *et al.* (1988); 5, Gilbert and Wiesel (1979); 6, Kisvárday *et al.* (1987); 7, Lin *et al.* (1979); 8, Martin (1988); 9, Ahmed *et al.* (1997).

recorded from 15 neurons *in vivo* that exhibited action potential characteristics very similar to FS cells identified *in vitro*. These cells displayed very brief action potentials, high maximum firing rates, a relative absence of spike frequency adaptation, large hyperpolarizing afterpotentials, and steep linear *f–I* relationships. Together these properties clearly distinguish them from other classes of cortical neurons such as regular spiking cells (McCormick *et al.*, 1985; Mason and Larkman, 1990), intrinsic bursting cells (Connors *et al.*, 1982; McCormick *et al.*, 1985; Connors and Gutnick, 1990), and chattering cells (Gray and McCormick, 1996; Azouz *et al.*, 1996). Our assumption that FS cells are inhibitory was supported by the recovery of three successfully stained cells, each of which was aspiny or sparsely spiny and of non-pyramidal morphology. One appeared to be similar to a 'clutch' cell of layer IV (Kisvárday *et al.*, 1985) while one of the other two neurons was a classic basket cell. Based upon the lateral axonal projections in the third cell, a small non-pyramidal cell in layer II, we suggest that this cell may also be a basket neuron, although this classification is only tentative. The intrinsic properties of these three cells showed no obvious differences when compared to the remaining 12 cells. Thus, our data are consistent with the interpretation that cells with FS characteristics are aspiny or sparsely spiny non-pyramidal neurons and are therefore inhibitory.

In addition to FS non-pyramidal cells, several groups have demonstrated that other non-pyramidal cells may exhibit electrophysiological features that are more similar to regular spiking neurons (Foehring *et al.*, 1991; Kawaguchi and Kubota, 1993, 1997; Thomson *et al.*, 1996; Thomson and Deuchars, 1997). To our knowledge, there have been no published reports demonstrating that cells with FS intrinsic properties, as outlined here, can have spiny pyramidal or spiny stellate morphology. These data therefore suggest that FS cells may represent only a fraction of the nine or more subclasses of morphologically and chemically distinct interneurons that have been identified in neocortex (Peters and Regidor, 1981; Fairen *et al.*, 1984; Jones and Hendry, 1984). Thus, not all cortical inhibitory interneurons have the intrinsic properties of FS cells, but our present knowledge strongly suggests that cells with FS properties are inhibitory.

Intrinsic and Visual Response Properties

The intrinsic response properties of FS cells display several striking characteristics that are likely to significantly shape their responses to visual stimuli. Their action potentials are very brief in duration and are followed by a prominent, but rapid, AHP. They show little or no evidence of spike frequency adaptation, and rarely exhibit long duration (slow) AHPs. As a result, these cells display a steep linear relation between firing rate and injected depolarizing current and are capable of firing at very high rates of discharge (Fig. 3, Table 1). This behavior suggests that these neurons may accurately relay the duration and intensity of their somatic input. Put another way, their output is capable of following strong and prolonged synaptic barrages, even at action potential discharge rates up to 500–600 Hz. Prior comparisons of the action potentials of regular spiking pyramidal cells and FS interneurons have demonstrated that the main difference between these cell types is the rapid rate of repolarization of the action potential in the FS cells (McCormick *et al.*, 1985). Direct examination of the Na$^+$ conductances involved in action potential generation have failed to find significant differences between pyramidal neurons and putative interneurons (Huguenard *et al.*, 1988). One possible difference between these cell types is that FS interneurons may possess a unique density, distribution, or kinetics and voltage dependence of the many subtypes of voltage and Ca^{2+}-dependent K$^+$ currents (Chen *et al.*, 1996b). The lack of spike frequency adaptation and the absence of a slow AHP in most FS cells implies a lack of sustained potassium conductances that could account for these phenomena.

The only novel feature seen in the intrinsic properties of these neurons, but not previously reported from *in vitro* results, was the slow depolarizing ramps preceding the fast upstroke of the action potentials (Fig. 2). This potential may be due to the activation of a persistent sodium current (I_{Nap}) (Stafstrom *et al.*, 1984, 1985; Llinas *et al.*, 1991). Similar effects of the persistent sodium current on unitary excitatory postsynaptic potentials (EPSPs) in quiescent pyramidal cells in layer III of rats during depolarization have been observed (Thomson *et al.*, 1988). This regenerative process may contribute substantially to the shortening of the ISI and consequently increase the firing rate

(Reyes *et al.*, 1993). Regardless of the biophysical mechanisms, FS neurons are capable of discharging with a broad range of frequencies in response to somatic polarization. Indeed, the injection of complex waveforms, including those that mimic the generation of PSPs during visual responses, reveal that the spike output of these neurons can exhibit a wide variety of interspike intervals in a reasonable representation of the frequency components present in the stimulus (Nowak *et al.*, 1997).

Consistent with their ability to generate a wide variety of frequencies, when stimulated with a drifting light bar, FS cells exhibited a unimodal ISIH with an approximate exponential decay (see Fig. 4*B*). The 'flat' ACHs and the lack of significant peaks in their corresponding power spectra further illustrate the lack of stereotyped repetitive activity in these neurons (Fig. 4). When stimulated with drifting square-wave gratings, these cells showed a greater tendency to generate action potentials at short interspike intervals (<5 ms). This enhancement of shorter interspike intervals may stem from a higher degree of activation of these neurons by the elevated luminance embedded in the gratings (Hess and Lillywhite, 1980), or by the distinct spatiotemporal receptive field interactions activated by the gratings and not the bars. However, the shorter interspike intervals did not significantly affect the form of the ACHs and the corresponding power spectra. Thus, unlike chattering cells (Gray and McCormick, 1996) and intrinsic bursting neurons (Connors *et al.*, 1982; McCormick *et al.*, 1985), these neurons do not appear to generate rhythmic bursts of action potentials through intrinsic mechanisms. Together, these properties suggest that the spike activity of FS cells 'linearly' conveys the sum of the currents arriving at the soma. The functional effect of their output will, of course, depend on several factors such as the release probability of the synapses, the postsynaptic receptors and conductance mechanisms and the integrative properties of the postsynaptic neurons (e.g. Thomson and Deuchars, 1997).

Interestingly, we found little evidence that FS neurons generate gamma frequency (20–70 Hz) oscillations in their action potential discharge during visual stimulation, despite speculation that GABAergic mechanisms may be critical to the generation of these oscillations (Llinás *et al.*, 1991; Bush and Douglas, 1991; Bush and Sejnowski, 1996; Jefferys *et al.*, 1996; Traub *et al.*, 1996). However, we cannot exclude a contribution of GABAergic mechanisms to the generation of gamma-band activity until several possible explanations are tested. There are many cells in visual cortex that fire at high rates of discharge and exhibit no evidence of periodicity (Gray *et al.*, 1990; Gray and Viana Di Prisco, 1997). Because our sample of cells was small, we could have easily under-sampled a subpopulation of interneurons that were oscillatory. Prior intracellular recordings in anesthetized cats have demonstrated clear fluctuations in the gamma frequency range in the membrane potential of chattering cells, a subtype of cortical pyramidal neuron (Gray and McCormick, 1996; Gray and Viana Di Prisco, 1997), suggesting that this pattern of activity may be limited to these cells. One possibility, however, is that other types of non-FS GABAergic neurons may contribute to the generation or modulation of gamma frequency oscillations and these remain to be recorded. The only oscillatory activity that we have yet observed in fast spiking neurons was a stimulus-locked 80 Hz oscillation in two cells, that may have arisen in response to the refresh 'flicker' of the computer monitor used to present visual stimuli.

Receptive Field Properties

Prior studies of the physiological responses of morphologically identified interneurons in the cat and primate primary visual cortex have revealed that they have varied receptive field properties (Table 4; Gilbert and Wiesel, 1979; Lin *et al.*, 1979; Kisvárday *et al.*, 1987; Martin *et al.*, 1983, 1989; Gabbott *et al.*, 1988; Martin, 1988; Anderson *et al.*, 1993; Ahmed *et al.*, 1997). Almost all of these intracellularly filled interneurons have been either basket, clutch or chandelier cells. The present study, along with those of other investigators (see Kawaguchi and Kubota, 1997), suggests that all of these morphological cell types may be FS in their intrinsic membrane properties. In agreement with the previous classifications of receptive field properties, we also found that FS interneurons in the cat primary visual cortex exhibit varied response properties (Table 3). Together, this sample of 14 morphologically identified cortical interneurons in the cat reveals that, like spiny stellate cells, GABAergic cells in layer IV are monocular and are typically 'simple' in their receptive field properties, although interneurons in layer IV that exhibit 'complex' receptive fields have also been observed (Table 4). Morphologically or physiologically identified interneurons outside of layer IV are typically binocular (Table 4), and may be either 'simple' or 'complex'. In our sample of FS neurons, most were binocular and simple in their receptive field properties, although one FS neuron exhibited receptive field responses of the complex type. The one FS cell that was filled with biocytin and located within layer IV appears morphologically similar to previously reported 'clutch' cells, which are a type of basket cell (Kisvárday *et al.*, 1985). This cell was monocular and exhibited simple receptive field properties, as previously reported for this type of neuron (Table 4).

Examination of the orientation tuning of our sample of FS neurons revealed that most were orientation selective with an orientation index that was similar to that of presumed pyramidal or spiny stellate cells (Maldonado and Gray, 1996; Maldonado *et al.*, 1997). In an effort to further evaluate whether FS interneurons are distinct from pyramidal cells in their orientation tuning, we compared the responses at the null orientation between the FS cells reported here and a sample of extracellularly recorded cells (n = 120, Maldonado and Gray, 1996). Interestingly, we found that even though most of the FS cells were orientation selective, five out of the eight cells in this study responded to all orientations. This observation is novel since it is not available in the studies described in Table 4. Examination of the literature concerning the orientation tuning of pyramidal cells revealed that very few studies have quantified whether cortical neurons exhibit minimal responses that are significantly different from their spontaneous activity. We therefore found it surprising that ~70% of extracellularly recorded cells (n = 120) in the anesthetized cat showed significant responses at their null orientation (mean = 18.9 ± 20.5% of the response to the preferred orientation; P.E. Maldonado and C.M. Gray, unpublished observation). These data indicate that the small sample of FS cells in this study are not distinct in their orientation tuning properties as compared to a larger sample of presumed pyramidal or spiny stellate cells. The significant minimal responses observed in the spike discharges of FS cells were further substantiated by the broad orientation tuning of the PSPs (Fig. 7). This indicates that FS interneurons may inhibit (or indirectly facilitate; Kisvárday *et al.*, 1993) their target pyramidal or spiny stellate cells, at all orientations.

Previous intracellular recordings from presumed cortical pyramidal or spiny stellate cells *in vivo* have demonstrated that IPSPs generated in simple cells exhibit orientation tuning that is parallel to that of the EPSPs recorded in the same neuron

(Ferster, 1986, 1988), although some investigators have provided evidence that the orientation tuning of GABAergic inputs is broader than that of the EPSPs (Morrone *et al.*, 1982; Ramoa *et al.*, 1986; Bonds, 1989). These findings are consistent with the local, dense axon collaterals of the FS neurons that we labeled (Fig. 1), as well as that previously shown for basket and chandelier cells (Martin *et al.*, 1983; Somogyi *et al.*, 1983; Kisvárday *et al.*, 1985; Freund *et al.*, 1983). Such strong local connections would be expected to give rise to iso-orientation inhibition, assuming that the orientation tuning of the GABAergic neurons was similar to that of the neighboring pyramidal or spiny stellate cells. The presence of extensive lateral projections in which the axon collaterals form synaptic contacts in regions of orientation preference that may vary considerably from that of the parent cell, however, also provides the opportunity for cross-orientation inhibition (Kisvárday *et al.*, 1994), as has been observed physiologically by some investigators (Volgushev *et al.*, 1993). Although these findings suggest that basket or FS interneurons may contribute to iso- or cross-orientation inhibition, this interpretation is complicated by the fact that these cells may synapse upon other inhibitory cells as well as pyramidal or spiny stellate neurons (Kisvárday *et al.*, 1993; Ahmed *et al.*, 1997).

Several models of the generation of orientation tuning in cortical neurons have been proposed and supported by experimental data (Sillito, 1984; Worgotter and Koch, 1991; Chapman and Stryker, 1992; Douglas *et al.*, 1995; Somers *et al.*, 1995; Vidyasagar *et al.*, 1996). It seems likely that, at least for simple cells, some degree of orientation tuning results from the alignment of afferents from thalamic neurons (Reid and Alonso, 1995; Chapmann *et al.*, 1991; Ferster, 1994; Ferster *et al.*, 1996), although this mechanism may be facilitated by the properties of recurrent excitatory collaterals and inhibitory mechanisms (Douglas *et al.*, 1995; Somers *et al.*, 1995). In this study we have revealed the relationship between the intrinsic and physiological response properties of FS interneurons in an effort to further understand the role of inhibition in shaping cortical activity. Although we are still far from a complete understanding of the network mechanisms of receptive field organization, particularly when we consider that there are many subtypes of GABAergic interneuron for which no physiological data are yet available, revealing the input–output relationships of local circuit and principal cells is one step in the elucidation of this network (e.g. Martin, 1988) and provides information to constrain and guide network models of visual cortical function.

Notes

References

Ahmed B, Anderson JC, Martin KAC, Nelson C (1997) Map of synapses onto layer 4 basket cells of the primary visual cortex of the cat. J Comp Neurol 380:230–242.

Albus K (1980) The detection of movement direction and effects of contrast reversal in the cat's striate cortex. Vision Res 20:289–293.

Anderson JC, Martin KAC, Whitteridge D (1993) Form function and intracortical projections of neurons in the striate cortex of the monkey *Macacus nemestrinus*. Cereb Cortex 3L:412–420.

Azouz R, Nowak LG, McCormick DA, Gray CM (1996) Multiparametric analysis of intracellular recording in the cat striate cortex reveal four distinct cell classes. Soc Neurosci Abstr 633:14.

Berman NJ, Douglas RJ, Martin KAC, Whitteridge D (1991) Mechanisms of inhibition in cat visual cortex. J Physiol 440:697–722.

Berman NJ, Douglas RJ, Martin KAC (1992) GABA-mediated inhibition in the neural networks of visual cortex. Progr Brain Res 90:443–476.

Bishop PO, Coombs JS, Henry GH (1971) Interaction effects of visual contours on the discharge frequency of simple striate neurones. J Physiol 219:659–687.

Bolz J, Gilbert CD (1986) Generation of end-inhibition in the visual cortex via interlaminar connections. Nature 320:362–365.

Bonds AB (1989) Role of inhibition in the specification of orientation selectivity of cells in the cat striate cortex. Vis Neurosci 2:41–55.

Bush P, Douglas RJ (1991) Synchronization of bursting action potential discharge in a model network of neocortical neurons. Neural Comput 3:19–30.

Bush P, Sejnowski T (1996) Inhibition synchronizes sparsely connected cortical neurons within and between columns in realistic network models. J Comp Neurosci 3:91–110.

Chapman B, Stryker MP (1992) Origin of orientation tuning in the visual cortex. Curr Opin Neurobiol 2:498–501.

Chapman B, Zahs KR, Stryker MP (1991) Relation of cortical cell orientation selectivity to alignment of receptive fields of the geniculocortical afferents that arborize within a single orientation column in ferret visual cortex. J Neurosci 11:1347–1358.

Chen W, Zhang J-J, Hu G-Y, Wu C-P (1996a) Electrophysiological and morphological properties of pyramidal and nonpyramidal neurons in the cat motor cortex *in vitro*. Neuroscience 73:39–55.

Chen W, Zhang J-J, Hu G-Y, Wu C-P (1996b) Different mechanisms underlying the repolarization of narrow and wide action potentials in pyramidal cells and interneurons of cat motor cortex. Neuroscience 73:57–68.

Connors BW, Gutnick MJ (1990) Intrinsic firing patterns of diverse neocortical neurons. Trends in Neuroscience 13:99–104.

Connors BW, Gutnick MJ, Prince DA (1982) Electrophysiological properties of neocortical neurons *in vitro*. J Neurophysiol 48:1302–1320.

Crook JM, Eysel UT (1992) GABA-induced inactivation of functionally characterized sites in the cat visual cortex (area 18): effects on orientation tuning. J Neurosci 12:1816–1826.

Crook JM, Eysel UT (1996) GABA-induced inactivation of functionally characterized sites in the cat visual cortex (area 18): effects on direction selectivity. J Neurophysiol 75:2071–2087.

DeFelipe J, Fairen A (1982) A type of basket cell in superficial layers of the cat visual cortex: a Golgi-electron microscope study. Brain Res 244:9–16.

Douglas RJ, Koch C, Mahowald M, Martin KAC, Suarez HH (1995) Recurrent excitation in neocortical circuits. Science 269:981–985.

Douglas RJ, Martin KAC, Whitteridge D (1988) Selective responses of visual cortical cells do not depend on shunting inhibition. Nature 332:642–644.

Douglas RJ, Martin KAC, Whitteridge D (1991) An intracellular analysis of the visual responses of neurons in cat visual cortex. J Physiol 440:659–696.

Engel AK, Roelfsema PR, Fries P, Brecht M, Singer W (1997) Role of the temporal domain for response selection and perceptual binding. Cereb Cortex 7:571–582.

Eysel UT (1992) Lateral inhibitory interactions in areas 17 and 18 of the cat visual cortex. Progr Brain Res 90:407–422.

Eysel UT, Crook JM, Machemer HF (1990) GABA-induced remote inactivation reveals cross-orientation inhibition in the cat striate cortex. Exp Brain Res 80:626–630.

Fairen A, DeFelipe J, Redigor J (1984) Nonpyramidal neurons: general account. In: Cerebral cortex, vol. 1, Cellular organization of the cerebral cortex (Peters A, Jones, EG, eds), pp 309–336. New York and London: Plenum Press.

Ferster D (1986) Orientation selectivity of synaptic potentials in neurons of cat primary visual cortex. J Neurosci 6:1284–1301.

Ferster D (1988) Spatially opponent excitation and inhibition in simple cells of the cat visual cortex. J Neurosci 8:1172–1180

Ferster D (1994) Linearity of synaptic interactions in the assembly of receptive fields in cat visual cortex. Curr Opin Neurobiol 4:563–568.

Ferster D, Chung S, Wheat H (1996) Orientation selectivity of thalamic input to simple cells of cat visual cortex. Nature 380:249–252.

Foehring RC, Lorenzon NM, Herron P, Wilson CJ (1991) Correlation of physiologically and morphologically identified neuronal types in human association cortex *in vitro*. J Neurophysiol 66:1825–1837.

Freeman WJ (ed.) (1975) Mass action in the nervous system. New York: Academic Press.

Freund TF, Martin KA, Smith AD, Somogyi P (1983) Glutamate decarboxylase-immunoreactive terminals of Golgi-impregnated axoaxonic cells and of presumed basket cells in synaptic contact with pyramidal neurons of the cat's visual cortex. J Comp Neurol 221:263–78

Gabbot PLA, Martin KAC, Whitteridge FRS (1988) Evidence for the connections between a clutch cell and a corticotectal neuron in area 17 of the cat visual cortex. Proc R Soc Lond B 233:385–391

Gilbert CD, Wiesel TN (1979) Morphology and intracortical projections of functionally characterized neurones in the cat visual cortex. Nature 280:120–215.

Gray CM (1994) Synchronous oscillations in neuronal systems: mechanisms and functions. J Comp Neurosci 1:11–38.

Gray CM, Singer W (1989) Stimulus-specific neuronal oscillations in orientation columns of cat visual cortex. Proc Natl Acad Sci USA 86:1698–1702.

Gray CM, McCormick DA (1996) Chattering cells: superficial pyramidal neurons contributing to the generation of synchronous oscillation in the visual cortex. Science 274:109–113.

Gray CM, Viana Di Prisco G (1997) Stimulus dependent neuronal oscillations and local synchronization in the striate cortex of the alert cat. J Neurosci 17:3239–3253.

Gray CM, Engel AK, Konig P, Singer W (1990) Stimulus-dependent neuronal oscillations in cat visual cortex: Receptive field properties and feature dependence. Eur J Neurosci 2:607–619.

Grieve KL, Sillito AM (1991) The length summation properties of layer VI cells in the visual cortex and hypercomplex cell end zone inhibition. Exp Brain Res, 84:319–325.

Hawken MJ, Parker AJ (1984) Contrast sensitivity and orientation selectivity in lamina IV of the striate cortex of Old World monkeys. Exp Brain Res 54:367–372.

Henry GH, Dreher B, Bishop PO (1974) Orientation specificity of cells in cat striate cortex. J Neurophysiol 37:1394–1409.

Hess RF, Lillywhite PG (1980) Effect of luminance on contrast coding in cat visual cortex. J Physiol 300:56–57p.

Hubel DH, Wiesel TN (1962) Receptive fields, binocular interaction and functional architecture in the cat's visual cortex. J Physiol Lond 160:106–154.

Huguenard JR, Hamill OP, Prince DA (1988) Developmental changes in Na$^+$ conductances in rat neocortical neurons: appearance of a slowly inactivating component. J Neurophysiol 59:778–795.

Jeffreys JG, Traub RD, Whittington MA (1996) Neuronal networks for induced '40 Hz' rhythms. Trends Neurosci 19:202–208.

Jones EG, Hendry SHC (1984) Basket cells. In: Cerebral cortex, vol. 1, Cellular organization of the cerebral cortex (Peters A, Jones, EG, eds), pp 309–336. New York and London: Plenum Press.

Jones RSG, Buhl EH (1993) Basket-like interneurones in layer II of the entorhinal cortex exhibit a powerful NMDA-mediated synaptic excitation. Neurosci Lett 149: 35–39.

Jones RSG, Heinemann U (1988) Synaptic and intrinsic responses of medial enthorinal cortical cells in normal and magnesium-free medium *in vitro*. J Neurophysiol 59:1476–1496.

Kawaguchi Y (1995) Physiological subgroups of nonpyramidal cells with specific morphological characteristics in layer II/III of rat frontal cortex. J Neurosci 15:2638–2655.

Kawaguchi Y, Kubota Y (1993) Correlation of physiological subgroupings of nonpyramidal cells with parvalbumin- and Calbindin$_{D28K}$-immunoreactive neurons in layer V of rat frontal cortex. J Neurophysiol 70:387–396.

Kawaguchi Y, Kubota Y (1996) Physiological and morphological identification of somatostatin- or vasoactive intestinal polypeptide-containing cells among GABAergic cell subtypes in rat frontal cortex. J Neurosci 16:2701–2715.

Kawaguchi Y, Kubota Y (1997) GABAergic cell subtypes and their synaptic connections in rat frontal cortex. Cereb Cortex 7:476–486.

Kisvárday ZF, Martin KAC, Whitteridge D, Somogyi P (1985) Synaptic connections of intracellularly filled clutch cells: a type of small basket cell in the visual cortex of the cat. J Comp Neurol 241:111–37.

Kisvárday ZF, Martin KAC, Friedlander MJ, Somogyi P (1987) Evidence for interlaminar inhibitory circuits in the striate cortex of the cat. J Comp Neurol 260:1–19.

Kisvárday ZF, Beaulieu C, Eysel UT (1993) Network of GABAergic large basket cells in cat visual cortex (area 18): Implication for lateral disinhibition. J Comp Neurol 327:398–415.

Kisvárday Z, Kim D-S, Eysel UT, Bonhoeffer T (1994) Relationship between lateral inhibitory connections and the topography of the orientation map in cat visual cortex. Eur J Neurosci 6:1619–1632.

Konig P, Schillen TB (1991) Stimulus-dependent assembly formation of oscillatory responses: I synchronization. Neural Comput 3:155–166.

Lin C-S, Friedlander MJ, Sherman SM (1979) Morphology of physiologically identified neurons in the visual cortex of the cat. Brain Res 172:344–348.

Llinás RR, Grace AA, Yarom Y (1991) *In vitro* neurons in mammalian cortical layer 4 exhibit intrinsic oscillatory activity in the 10- to 50-Hz frequency range. Proc Natl Acad Sci 88:897–901.

Lytton W, Sejnowski TJ (1991) Simulations of cortical pyramidal neurons synchronized by inhibitory interneurons. J Neurophysiol 66:1059–1079.

Maffei L, Fiorentini A (1973) The visual cortex as a spatial frequency analyser. Vis Res 13:1255–1267.

Maldonado PE, Gray CM (1996) Heterogeneity in local distributions of orientation-selective neurons in the cat primary visual cortex. Vis Neurosci 13:509–513.

Maldonado PE, Godecke I, Gray CM, Bonhoeffer T (1997) Orientation preference in pinwheel centers in cat striate cortex. Science 276:1551–1555.

Martin KAC (1984) Neuronal circuits in cat striate cortex In: Cerebral cortex, vol. 2, Functional properties of cortical cells (Peters A, Jones, EG, eds), pp 241–284. New York and London: Plenum Press.

Martin KAC (1988) From single cells to simple circuits in the cerebral cortex. Q J Exp Physiol 73:637–702.

Martin KAC, Somogyi P, Whitteridge D (1983) Physiological and morphological properties of identified Basket cells in the cat's visual cortex. Exp Brain Res 50:193–200.

Martin KAC, Friedlander MJ, Alones V (1989) Physiological morphological and cytochemical characteristics of a layer I neuron in cat striate cortex. J Comp Neurol 282:404–414.

Mason A, Larkman A (1990) correlation between morphology and electrophysiology of pyramidal neurons in slices of rat visual cortex, II. Electrophysiology. J Neurosci 10:1415–1428.

McCormick DA, Connors BW, Lighthall JW, Prince DA (1985) Comparative electrophysiology of pyramidal and sparsely spiny stellate neurons of the neocortex. J Neurophysiol 54:782–806.

Morrone MC, Burr DC, Maffei L (1982) Functional implication of cross-orientation inhibition of cortical visual cells Neurophysiological evidence. Proc R Soc Lond Biol 216:335–354.

Movshon JA, Thompson ID, Tolhurst DJ (1978a) Spatial sommation in the receptive fields of simple cells in the cat's striate cortex. J Physiol 283:53–77.

Movshon JA, Thompson ID, Tolhurst DJ (1978b) Recpetive field organization of complex cells in the cat's striate cortex. J Physiol 283:79–99.

Naegele JR, Katz LC, (1990) Cell surface molecules containing *N*-acetylgalactosamine are associated with basket cells and neurogliaform cells in cat visual cortex. J Neurosci 10:540–557.

Nowak LG, Sanchez-Vives MV, McCormick DA (1997) The influence of low and high frequencies on spike timing in the visual cortex. Cereb Cortex 7:487–501.

Orban GA (1984) Neural operations in the visual cortex. Berlin: Springer-Verlag.

Orban GA, Kato H, Bishop PO (1979) End-zone region in receptive fields of hypercomplex and other striate neurons in the cat. J Neurophysiol 42:818–32.

Peters A, Regidor J (1981) A reassessment of the forms of nonpyramidal neurons in area 17 of cat visual cortex. J Comp Neurol 203:685–716.

Press WM, Flannery BP, Teukolsky SA, Vetterling WT (1992) Numerical recipes in C: the art of scientific computing. Cambridge: Cambridge University Press.

Ramoa AS, Shadlen M, Skottun BC, Freeman RD (1986) A comparison of inhibition in orientation and spatial frequency selectivity of cat visual cortex. Nature 321:237–239.

Reid RC, Alonso JM (1995) Specificity of monosynaptic connections from thalamus to visual cortex. Nature 378:281–284.

Reyes AD, Fetz EE (1993) Two modes of interspike interval shortening by brief transient depolarizations in cat neocortical neurons. J Neurophysiol 69:1661–1672.

Sillito AM (1977) Inhibitory processes underlying direction specificity of simple complex and hypercomplex cells in the cat's visual cortex. J Physiol 271:299–320.

Sillito AM (1984) Functional considerations of the operation of GABAergic inhibitory processes in the visual cortex. In: Cerebral cortex, vol. 2, Functional properties of cortical cells (Peters A, Jones, EG, eds), pp 91–118. New York and London: Plenum Press.

Singer W, Gray CM (1995) Visual feature integration and the temporal correlation hypothesis. Annu Rev Neurosci 18:555–586.

Skottun BC, De Valois RL, Grosof DH, Movshon JA, Albrecht DG, Bonds AB (1991) Classifying simple and complex cells on the basis of response modulation. Vis Res 31:1079–86.

Somers DC, Nelson SB, Sur M (1995) An emergent model of orientation selectivity in cat visual cortical simple cells. J Neurosci 15:5448–5465.

Somogyi P, Kisvárday ZF, Martin KAC, Whitteridge D (1983) Synaptic connections of morphologically identified and physiologically characterized large basket cells in the striate cortex of cat. Neuroscience 10:261–294.

Swadlow H A (1988) Efferent neurons and suspected interneurons in binocular visual cortex of the awake rabbit: receptive field and binocular properties. J Neurophysiol 59:1162–1187.

Stafstrom CE, Schwindt PC, Flatman JA, Crill WE (1984) Properties of subthreshold response and action potential recorded in layer V neurons from cat sensorimotor cortex in vitro. J Neurophys 52:244–263.

Stafstrom CE, Schwindt PC, Chubb MC, Crill WE (1985) Properties of persistent sodium conductances and calcium conductance of layer V neurons from cat sensorimotor cortex in vitro. J Neurophys 53:153–169.

Tasker JG, Hoffman NW, Kim YI, Fisher RS, Peacock WJ, Dudek FE (1996) Electrical properties of neocortical neurons in slices from children with intractable epilepsy. J Neurophysiol 75:931–939.

Thomson AM, Deuchars J (1997) Synaptic interactions in neocortical local circuits: dual intracellular recordings in vitro. Cereb Cortex 7:510–522.

Thomson AM, Girdlestone D, West DC (1988) Voltage-dependent currents prolong single axon postsynaptic potentials in layer III pyramidal neurons in rat neocortical slices. J Neurophysiol 60:1896–1907.

Thomson AM, West DC, Deuchars J (1996) Single axon IPSPs elicited in pyramidal cells by three classes of interneurones in slices of rat neocortex. J Physiol 496:81–102.

Traub RD, Whittington MA, Stanford IM, Jefferys JG (1996) A mechanism for generation of long-range synchronous fast oscillations in the cortex. Nature 383:621–624.

Vidyasagar TR, Pei X, Volgushev M (1996) Multiple mechanisms underlying the orientation selectivity of visual cortical neurones. Trends Neurosci 19:272–272.

Volgushev M, Pei X, Vidyasagar TR, Creutzfeldt OD (1993) Excitation and inhibition in orientation selectivity of cat visual cortex neurons revealed by whole-cell recordings in vitro. Vis Neurosci 10:1151–1155.

Watkins DW, Berkley MA (1974) The orientation selectivity of single neurons in cat striate cortex. Exp Brain Res 19:433–446.

Wilson HR, Cowan JD (1972) Excitatory and inhibitory interactions in localized populations of model neurons. Biophys J 12:1–24.

Worgotter F, Koch C (1991) A detailed model of the primary visual pathway in the cat: comparison of afferent excitatory and intracortical inhibitory connection schemes for orientation selectivity. J Neurosci 11:1959–1979.